

Supporting Information

In situ confined synthesis of interlayer-riveted carbon shell encapsulated PdZnBi alloy as highly active and durable oxygen reduction reaction catalyst

LiYuan Chang^a, KaiLing Zhou^a, WeiHan Si^a, Chao Wang^a, ChangHao Wang^{*a}, ManChen Zhang^b,
XiaoXing Ke^b, Ge Chen^{*c} and RuZhi Wang^{*a}

Email address: wrz@bjut.edu.cn; chenge@bjut.edu.cn; wangch33@bjut.edu.cn

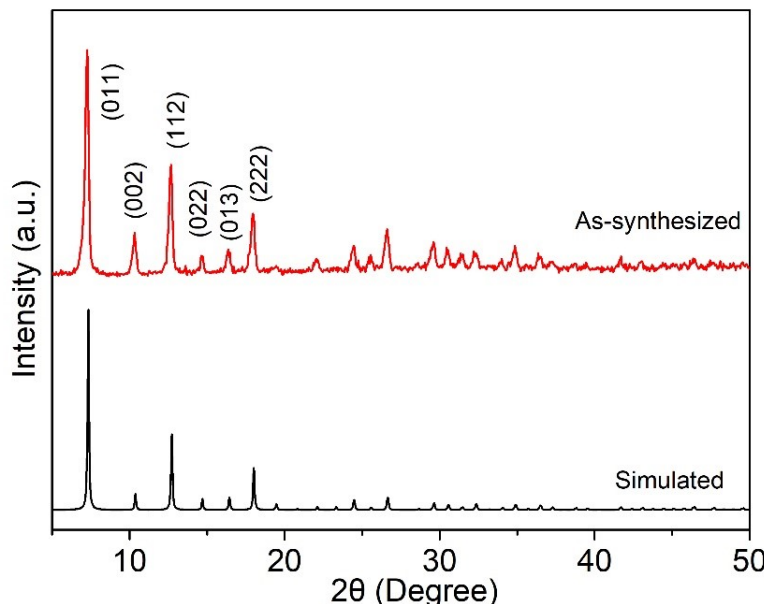


Fig. S1. XRD spectra of synthetic ZIF-8

* Corresponding author. Email address: wrz@bjut.edu.cn; chenge@bjut.edu.cn; wangch33@bjut.edu.cn

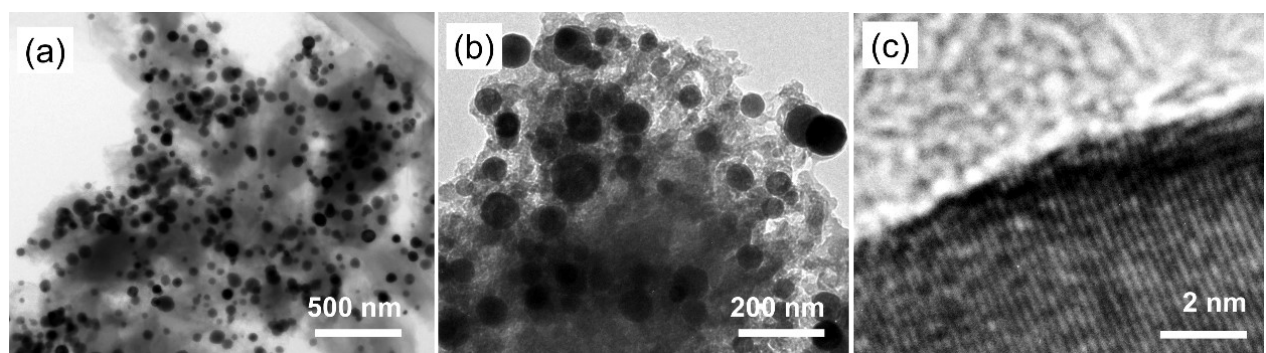


Fig. S2. TEM images of PdZnBi/NC-SL at different magnification

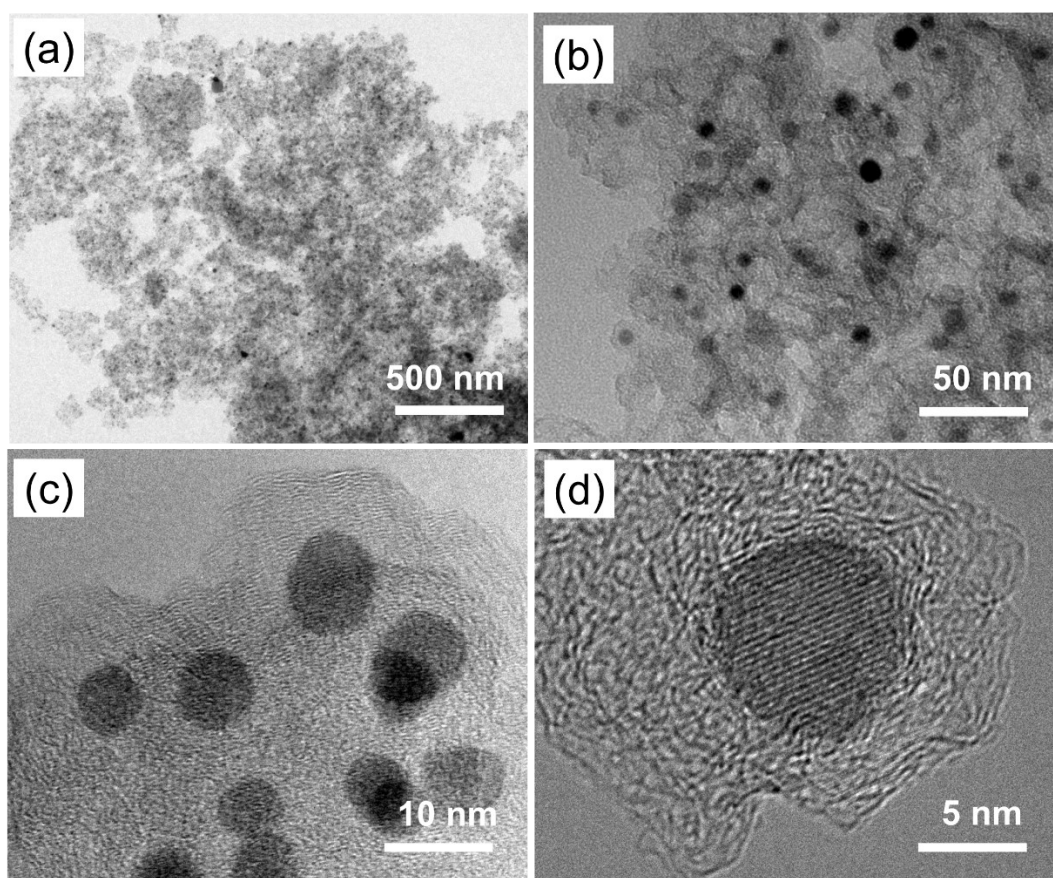


Fig. S3. PdZnBi/NC-IR TEM images with different magnifications

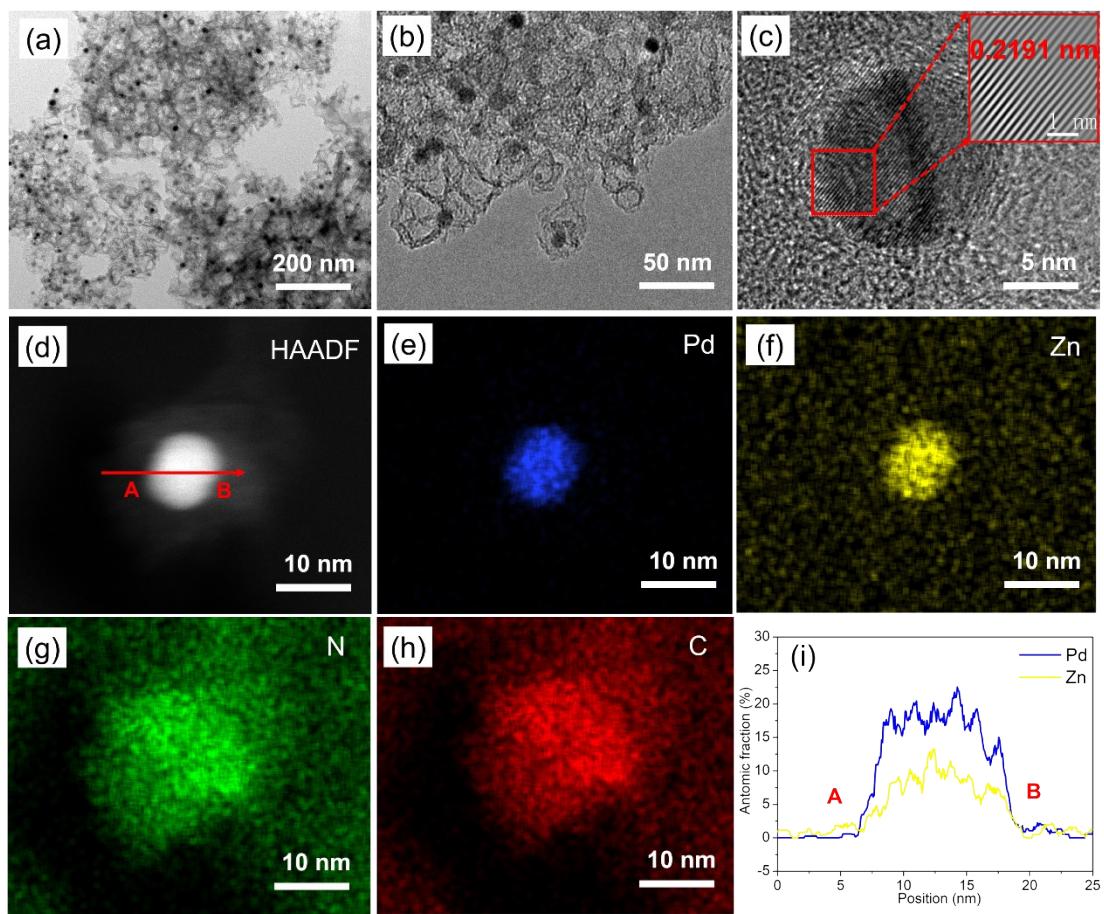


Fig. S4. (a~c) TEM images of PdZn/NC-IR at different magnification; (d) HAADF-STEM image of PdZn/NC-IR; (e~h) Elemental mappings of PdZn/NC-IR; (i) Line scan corresponding to the red arrow in Fig. (d).

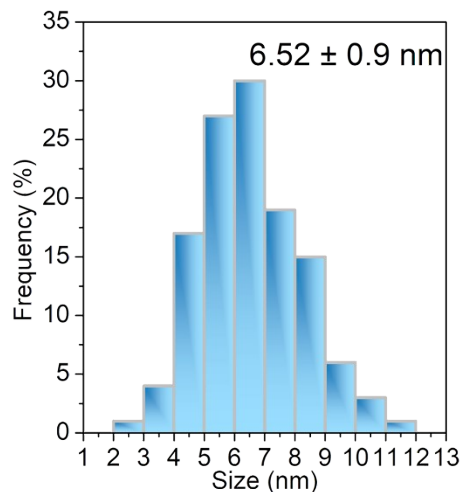


Fig. S5. Particle size distribution of PdZn/NC-IR;

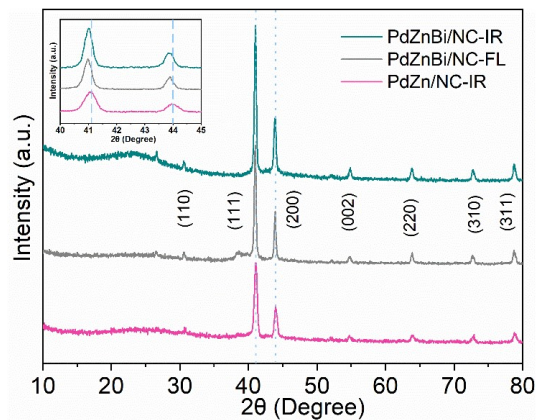


Fig. S6. XRD pattern of PdZnBi/NC-SL, PdZn/NC-IR and PdZnBi/NC-IR and Local enlargement

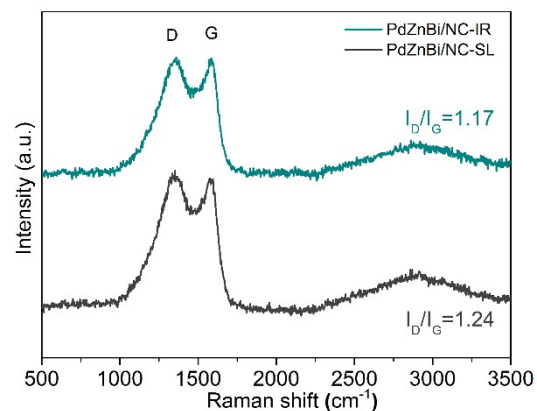


Fig. S7. Raman curve of PdZnBi/NC-IR and PdZnBi/NC-SL

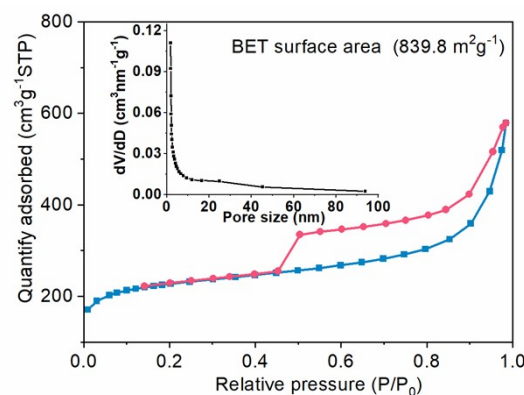


Fig. S8. N₂ adsorption-desorption isotherms of PdZnBi/NC-IR, the inset showing the corresponding pore size distribution

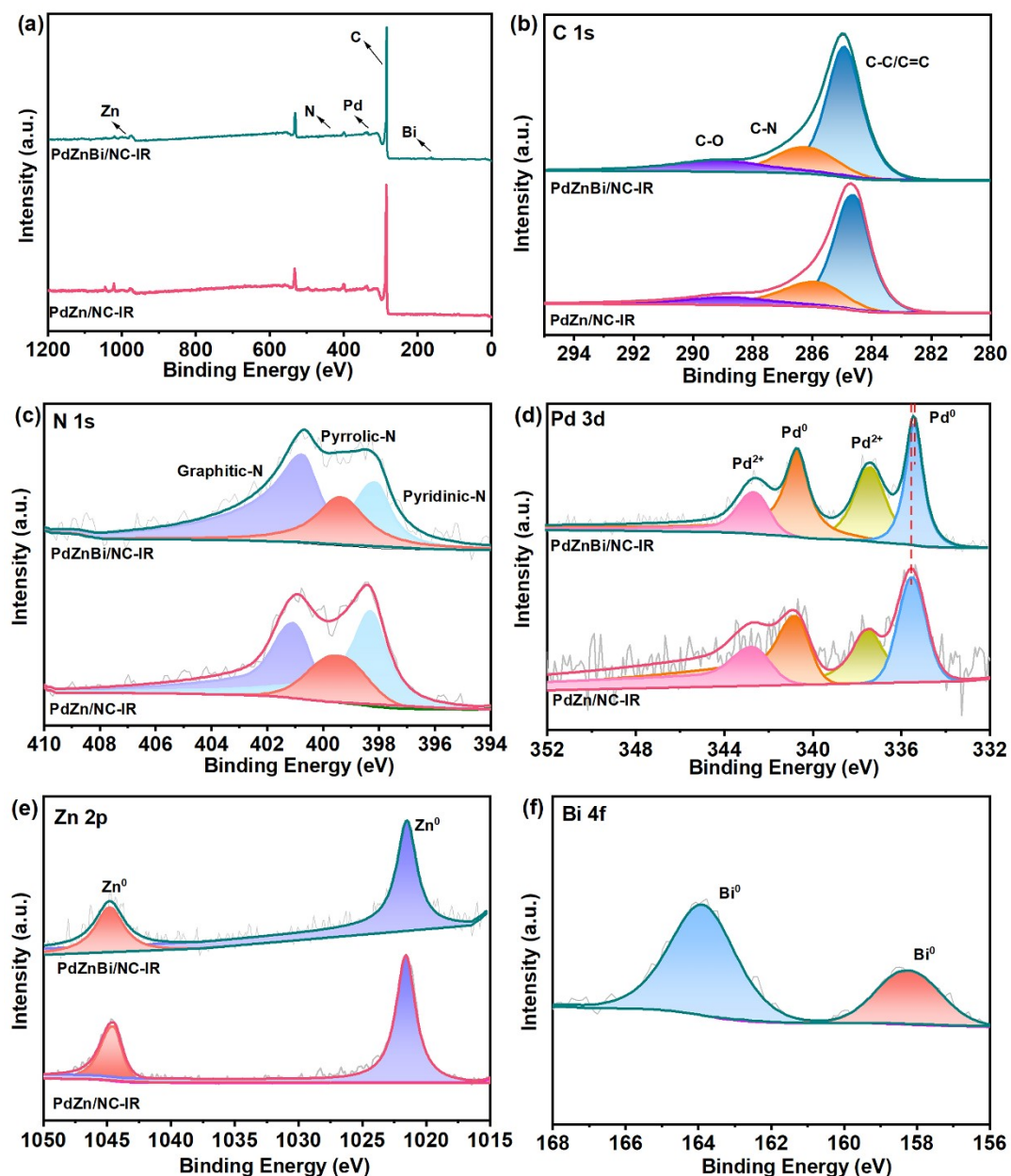


Fig. S9. XPS spectra of PdZn/NC-IR and PdZnBi/NC-IR. (a) Full survey spectra and deconvoluted (b) Pd 3d (c) N 1s, (d) C 1s, (e) Zn 2p and (f) Bi 4f spectra.

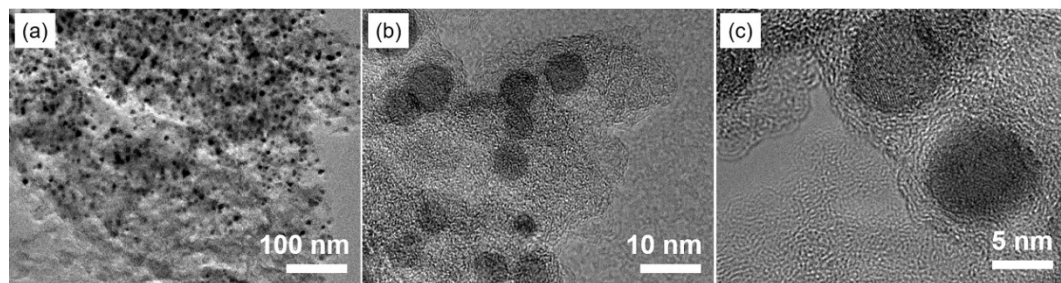


Fig. S10. PdZn alloy synthesized by sodium acetate as an additive.

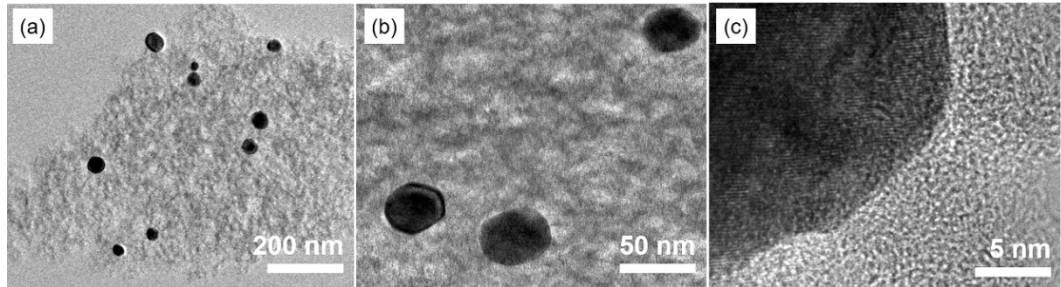


Fig. S11. PdZn alloy synthesized by glucose as an additive.

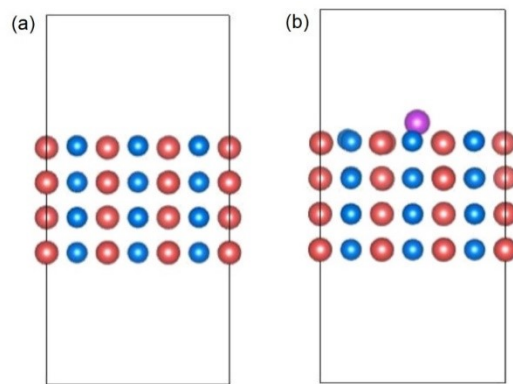


Fig. S12. (a) PdZn (111) and (b) PdZnBi (111). The red sphere represents the Pd atom, the blue sphere represents the Zn atom, and the purple sphere represents the Bi atomic

table.

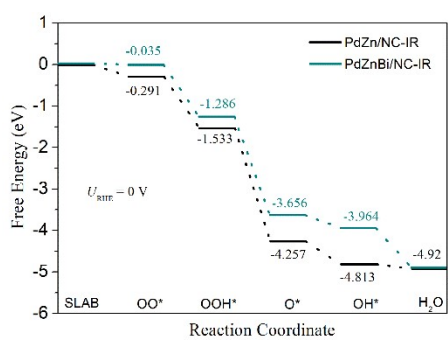


Fig. S13. Free energy diagrams of ORR on PdZn/NC-IR and PdZnBi/NC-IR at 0 V.

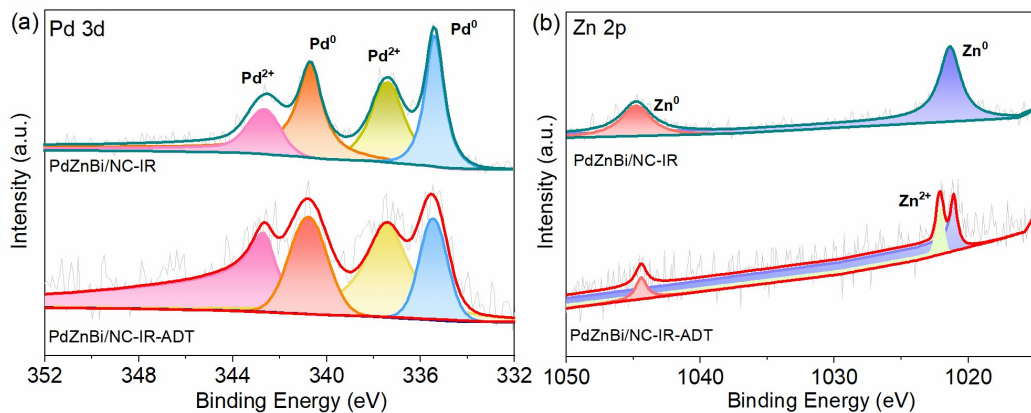


Fig. S14. XPS spectra of PdZnBi/NC-IR catalyst before and after stability test: (a) Pd 3d, (b) Zn 2p

Table S1. Elemental content in PdZnBi/NC-IR

Elemental	Values (ppm)
Pd	5.068
Zn	5.591
Bi	0.634

Table S2. Elemental content in PdZn/NC-IR

Elemental	Values (ppm)
Pd	5.235
Zn	5.712

Table S3. Elemental content in PdZnBi/NC-SL

Elemental	Values (ppm)
Pd	5.149
Zn	5.683
Bi	0.705

Table S4. Performance of samples

samples	E _{1/2} (V)	MA (A mg ⁻²)	SA (mA cm ⁻²)
Pt/C	0.862	0.087	0.13
Pd/C	0.813	0.07	0.34
PdZnBi/NC-SL	0.808	0.10	0.14
PdZn/NC-IR	0.883	0.78	0.71
PdZnBi/NC-IR	0.892	1.05	0.73

Table S5. Bard charge of four atoms around Bi in PdZnBi/NC-IR

Atom	Charge (e)	Transferred charge (e)
Bi	4.6588	-0.3412
1-Pd	10. 4170	+0. 4170
2-Pd	10. 4170	+0. 4170
3-Pd	10. 4012	+0. 4012
4-Pd	10. 4012	+0. 4012

Table S6. Comparison of stability

Catalyst	Number of cycles (k)	Mass activity retention rate (%)	Ref.
Pd/p-BNO	5	93.9	[48]
Pd ₃ Bi	10	71	[14]
Pt/TiO ₂ -C	10	71.2	[49]
Pd ₅ Bi ₂ /C	10	74	[50]
FePt@PtBi	10	82	[51]
PtCo/C	10	87	[52]
Pd–N–C	10	90	[53]
Pd ₁₇ Se ₁₅ NPs/C	15	55.5	[54]
Pd ₅₉ Cu ₃₀ Co ₁₁	15	68.4	[55]
Pd/NRGO	15	72	[56]
Pt ₃ Co _{0.6} Ti _{0.4} /DMC	15	78.5	[57]
HD-PdZn	20	79.9	[58]
PtCuAu _{0.0005} /C	20	83	[59]
PdMo bimettallene	30	72	[13]
PtCo-PtSn/C	30	72.6	[60]
Au-O-PdZn	30	90.5	[17]
nt-PtNiN/KB	30	72.7	[61]
Pt ₇₈ Zn ₂₂	30	85	[62]
Pt ₂ CuW _{0.25} /C	30	90.9	[63]
Pt ₃ Co@Pt-SAC	50	90	[64]
This work	60	84	-